A Quasi-TEM Analysis for Curved and Straight Planar Multiconductor Systems

HEINRICH DIESTEL

Abstract — **In this paper an extended quasi-TEM analysis is presented. The transverse field of the weakly curved planar multiconductor system is described by the static electric and magnetic solutions of the corresponding axially symmetrical structure. The capacitance and inductance matrices of this system of concentric microstrip rings are calculated using the "method of lines." A two-port network consisting of circularly curved transmission lines is calculated and the results are compared with measured values.**

I. Introduction

AT LOW FREQUENCIES the dimensions of planar transmission lines, e.g. for delay lines and directional couplers, represent a serious problem. In many cases the lines are curved, in order to satisfy the small-size requirements of the system packaging, and the radii of curvature are chosen large to keep losses as small as possible. Because of the long wavelengths the electromagnetic field is extremely extended, so that all parts of the circuit are coupled and parasitic effects can become dominant.

A rigorous analysis of such networks with straight and curved planar multiconductor systems has not yet been given. Since waveguide curvature represents a rather involved mathematical problem, analytical methods are available for only a few simple curved structures [1], [2].

Most of the procedures concerned with curvature make certain simplifying assumptions, e.g. that the curved segment of waveguide may be considered part of an infinite circular spiral [3]. This approximation has been applied successfully to the groove [4] and to the dielectric waveguide [5] and has been adopted for the present analysis.

The fundamental modes of straight planar multiconductor systems are pure TEM only for the case of lossless strip lines in a homogeneous dielectric. If the dielectric is layered the guided waves are hybrid; i.e., longitudinal field components also exist. In the theory of quasi-TEM modes these components, which are small at low frequencies, are neglected and the transverse field is approximated by a composition of static electric and static magnetic fields.

If curvature is introduced to the multiconductor system (Fig. 1), the dominant structure of the electromagnetic field does not change abruptly. For moderate curvature the main field components are furthermore perpendicular to the curved axis; i.e., the propagating modes are basically of the TEM kind [5], [6].

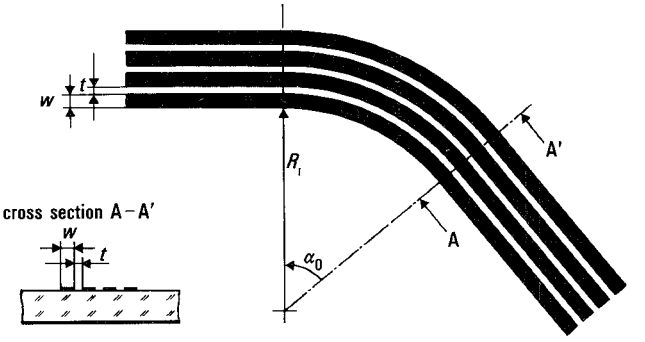

Fig. 1. Top and cross-sectional views of a planar multiconductor system with sections of straight and circularly curved coupled transmission lines

In the present paper the transmission properties of circularly curved multiconductor systems are described by currents and voltages, as in the case of straight guides [7]. The propagation constants result from the solution of a real eigenvalue problem with static capacitance and inductance matrices. In the limiting case of zero frequency, the transverse electromagnetic field of the section of curved lines approximately coincides with the static electric and magnetic solutions of the corresponding axially symmetrical structure. The two static field problems of the system of concentric ring lines are solved accurately and in a uniform manner in this paper.

If curvature is reduced, the curved system of guides converges to the corresponding straight one. The method presented here can follow this process of reduction steadily, including the transition to straight conductors. It is therefore also possible to correctly consider very weak curvature, which cannot be achieved by methods with fundamentally different expansion functions for curved and straight guides.

II. Analysis

In the quasi-TEM analysis the transverse electromagnetic field is described by a combination of static electric and magnetic fields.

From Maxwell's equations the following relations for the electrostatic field of the axially symmetrical structure

Manuscript received May 31, 1988; revised November 3, 1988.

The author is with the Bereich Uebertragungstechnik, Siemens AG, Hofmannstrasse 51, D-8000 Munich, West Germany.

IEEE Log Number 8826036.

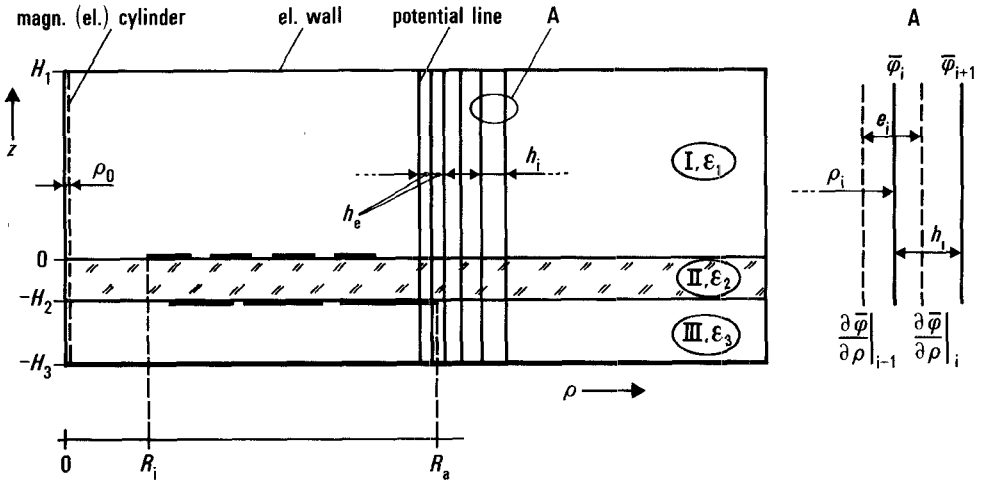

Fig. 2. Cross-sectional view of concentric microstrip rings at different interfaces. The inner and outer radii of the total multiconductor system are given by R_i and R_a. In detail A the lines of discretization for the potential function $\bar{\varphi} = \bar{\varphi}^{E(H)}$ and its first derivative are sketched; e_i and h_i denote interval sizes ($e_i = h_i = h$ for equidistant discretization) and ρ_i is the radial distance to the ith potential line. Near the strip edges the intervals are equal in size and have the small value $h_i = h_e$.

result:

$$\nabla \times \vec{E}(\rho, z) = 0 \qquad \nabla(\epsilon \vec{E}) = \sigma(\rho, z) \tag{1}$$

where $\sigma(\rho, z)$ gives the surface charge density. Equations (1) represent a two-dimensional potential problem with a scalar potential function $\varphi^E(\rho, z)$, which must satisfy Laplace's differential equation in the cylindrical (ρ, α, z) coordinate system:

$$\frac{\partial^2\varphi^E}{\partial z^2} + \frac{\partial^2\varphi^E}{\partial\rho^2} + \frac{1}{\rho}\frac{\partial\varphi^E}{\partial\rho} = 0. \tag{2}$$

Dirichlet's condition holds for shielding electric walls, and at $\rho = 0$ Neumann's condition

$$\frac{\partial\varphi^E}{\partial\rho} = 0 \tag{3}$$

must be considered.

In the following this boundary value problem is solved in the same manner and hence with the same accuracy as the boundary value problem for the static magnetic field, which from Maxwell's equations is defined by

$$\nabla \times \vec{H}(\rho, z) = \vec{j} \qquad \nabla(\mu_0 \vec{H}) = 0 \tag{4}$$

with the electrical current density $\vec{j} = j(\rho, z)\vec{e}_\alpha$. The magnetic field strength $\vec{H}$ can be derived from a solenoidal vector potential, $\vec{A} = \varphi^H(\rho, z)\vec{e}_\alpha$, which is a solution of the partial differential equation

$$\frac{\partial^2\varphi^H}{\partial z^2} + \frac{\partial^2\varphi^H}{\partial\rho^2} + \frac{1}{\rho}\frac{\partial\varphi^H}{\partial\rho} - \frac{1}{\rho^2}\varphi^H = 0. \tag{5}$$

At a sufficient distance on the shielding electric walls the potential function is given by

$$\varphi^H = 0. \tag{6}$$

This boundary condition is also valid on the metallized ground plane and is generated in certain methods by mirror currents. In contrast to the electrostatic problem, where (3) holds at $\rho = 0$, the magnetic vector potential on the coordinate axis is determined by (6). This can be deduced from the behavior of the potential function in the limit $\rho \to 0$ if circular filamentary currents are assumed [8].

The static electric and magnetic field problems are solved in the following using the semianalytical "method of lines" [9]–[13]. For this purpose a simple transformation of the two potential functions is performed:

$$\bar{\varphi}^{E(H)} = \sqrt{\rho/\bar{\rho}}\,\varphi^{E(H)} \tag{7}$$

where $\bar{\rho}$ denotes a mean radius, defined below.

After transformation the partial differential equations for the scalar and vector potential functions take the form

$$\frac{\partial^2\bar{\varphi}^{E(H)}}{\partial z^2} + \frac{\partial^2\bar{\varphi}^{E(H)}}{\partial\rho^2} + \frac{c^{E(H)}}{\rho^2}\bar{\varphi}^{E(H)} = 0 \tag{8}$$

with the constants $c^E = 1/4$ and $c^H = -3/4$.

At the interfaces of the dielectric regions in Fig. 2 are striplines of zero thickness. Because of the field singularities at the strip edges the ρ dependence of the potential functions is very complicated, so that an analytical solution with Bessel and trigonometric expansion functions becomes extremely cumbersome.

The semianalytical method of lines bypasses the difficulties caused by the strip edges. In the ρ direction, where field singularities occur, a discrete description of the functions is chosen, whereas in the z direction the fields are expressed analytically.

On the axis $\rho = 0$ the derivatives of the transformed potential function $\bar{\varphi}^E$ exhibit singular behavior. The z axis is therefore excluded for both potential functions, and on a cylindrical wall with a small radius ρ_0 (Fig. 2) we have boundary conditions which are derived from (3) and (6). All other ideal boundaries uniformly require Dirichlet's condition $\bar{\varphi}^{E(H)} = 0$.

The potential functions are discretized in order to solve the partial differential equations (8) using the method of lines. A good first approximation for an optimal discretiza-

tion is given in [12] for straight waveguides and this discretization is well suited also for circularly curved striplines (cf. [13]).

After two simple intermediate transformations, called normalization, one obtains the following systems of M coupled ordinary differential equations:

$$\frac{d^2}{dz^2}\vec{\Phi}^{E(H)} + \frac{1}{h^2}\left[D_{\rho\rho}^{E(H)}\right]\vec{\Phi}^{E(H)} + c^{E(H)}[\rho]^{-2}\vec{\Phi}^{E(H)} = \vec{0} \tag{9}$$

with the normalized potentials $\vec{\Phi}_{(z)}^{E(H)} = [r_e]^{-1}\vec{\varphi}_{(z)}^{E(H)}$. The diagonal matrix $[r_e] = \mathrm{diag}(\sqrt{h/e_t})$ is a function of the interval sizes e_t and h (Fig. 2, detail), and the vector

$$\vec{\bar{\varphi}}^{E(H)} = \left(\frac{\varphi_1^{E(H)}}{\sqrt{\bar{\rho}/\rho_1}}, \cdots, \frac{\varphi_M^{E(H)}}{\sqrt{\bar{\rho}/\rho_M}}\right)^t = [r]^{-1}\vec{\varphi}^{E(H)} \tag{10}$$

depends on the potentials in the original domain:

$$\vec{\varphi}_{(z)}^{E(H)} = \left(\varphi_1^{E(H)}(z), \cdots, \varphi_M^{E(H)}(z)\right)^t.$$

The diagonal matrix $[r] = \mathrm{diag}(\sqrt{\bar{\rho}/\rho_t})$ has a particular meaning. Since the curvature of a circle is equal to the reciprocal radius, the ith element of $[r]^2$ denotes the normalized curvature of the waveguide at the ith line. The radial distances to the lines of discretization are given by $[\rho] = \mathrm{diag}\,(\rho_t)$.

In principle the mean radius $\bar{\rho}$ can be chosen arbitrarily. In what follows $\bar{\rho}$ is given by the value $(R_t + R_a)/2$ where R_t and R_a are the radial distances of the outer strip edges, as illustrated in Fig. 2.

Because of different lateral boundary conditions for the two potential functions, denoted by E and H, we have different second-order operators

$$\left[D_{\rho\rho}^{E(H)}\right] = -\left[D_{\rho}^{E(H)}\right]^t\left[D_{\rho}^{E(H)}\right].$$

By orthogonal transformation the systems of M coupled differential equations (9) can be decoupled, and one obtains

$$\frac{d^2}{dz^2}\vec{V}^{E(H)} - \left[\chi^{E(H)}/h\right]^2\vec{V}^{E(H)} = \vec{0} \tag{11}$$

with the vectors of transformed potentials $\vec{V}^{E(H)}(z) = [T_{E(H)}]^t\vec{\Phi}_{(z)}^{E(H)}$ and the real, positive, and distinct eigenvalues $\chi_j^{E(H)}/h$. The general solutions of (11) correspond to the simple transmission line equations.

In the following the problem of two dielectric layers with striplines at the interface is treated in order to make a comparison with [12] (Fig. 2, $H_3 = H_2$).

As mentioned above, the tangential electric field must vanish at the coordinate planes $z = (\pm)H_{1(2)}$. Continuity conditions must be considered at $z = 0$, so that the normalized electrostatic potential is related to the charge at the interface as follows:

$$\vec{\Phi}^E(0) = [T_E]\,\mathrm{diag}\left(1/c_j\right)[T_E]^t\vec{Q}_s = [\Gamma_E]\vec{Q}_s \tag{12}$$

with

$$c_j/\epsilon_0 = \chi_j^E\left(\epsilon_{r1}\coth\left(\chi_j^E H_1/h\right) + \epsilon_{r2}\coth\left(\chi_j^E H_2/h\right)\right) \tag{13}$$

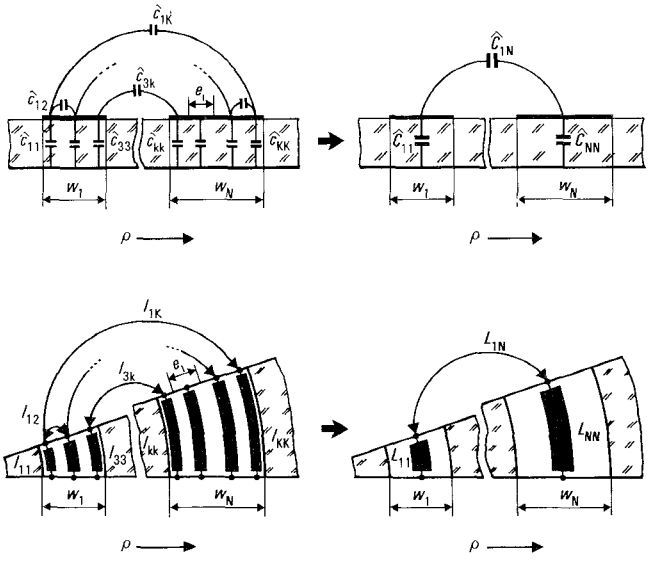

Fig. 3. The ring widths w_1 to w_N are subdivided into microrings of the radial widths e_t. (a) The microcapacitances $\hat{c}_{ik} = (\hat{c}_{ik})_s \cdot s$ are summed to the macrocapacitances $\hat{C}_{mn} = (\hat{C}_{mn})_s \cdot s$ for the N circular striplines. (b) For the same structure as in (a) the microinductances $l_{ik} = (l_{ik})_s \cdot s$ are summed to the macroinductances $L_{mn} = (L_{mn})_s \cdot s$.

and the normalized vector of charge,

$$\vec{Q}_s = [r_e][r]\vec{q}_s. \tag{14}$$

The subscript s refers to differentiation with respect to the variable $s = \bar{\rho}\alpha$.

In (12) only those elements of the matrix $[\Gamma_E]$ belonging to striplines are evaluated. These elements can be given explicitly and form the real and symmetric "reduced" matrix in the normalized domain [12].

After transformation into the original domain and inversion of the matrix, the following equation is derived:

$$\left(\vec{q}_s\right)_{\mathrm{red}} = \left([r][r_e][\Gamma_E][r_e][r]\right)_{\mathrm{red}}^{-1}\vec{\varphi}_{\mathrm{red}}^E = [c_s]\vec{\varphi}_{\mathrm{red}}^E. \tag{15}$$

The elements dc_{ik}/ds of the real and symmetric matrix $[c_s]$ represent microcapacitances with respect to the length $ds = \bar{\rho}\,d\alpha$. As illustrated in Fig. 3(a), the capacitances $\hat{c}_{ik}$, defined by $\hat{c}_{ik} = -c_{ik}$, if $i \neq k$, and $\hat{c}_{ii} = \sum_{k=1}^{K} c_{ik}$, form a dense network with microrings of widths e_t.

The macrocapacitances for the circular striplines of widths w_n result from the summation of the corresponding microcapacitances; one obtains

$$\vec{q}' = [C_s]\vec{u} \tag{16}$$

with the charges per unit length $\vec{q}' = (q_s^{(1)}, \cdots, q_s^{(N)})^t$ and the potentials $\vec{u} = (u^{(1)}, \cdots, u^{(N)})^t$ for the N planar conductors.

The static electric and the static magnetic fields represent independent solutions of Maxwell's equations. With the present method both field-theoretical problems can be solved accurately and in a uniform manner.

The continuity of the transformed magnetic potential $V_j^H(z)$ at the interface follows from the continuity of the normal magnetic induction. The magnetic flux at $z = 0$ is related to the vector potential by the equation

$$\vec{\theta}_s(0) = [r_e]^{-1}[r]\vec{\vartheta}_s = \vec{\Phi}^H(0) \tag{17}$$

where $\vec{\theta}_s$ gives the vector of normalized magnetic flux with respect to the length ds.

Matching of the tangential magnetic field strength then leads to the equation

$$\vec{\theta}_s(0) = [T_H]\,\mathrm{diag}(l_j)[T_H]^t\vec{I} = [\Gamma_H]\vec{I} \qquad (18)$$

with the elements of the diagonal matrix

$$l_j/\mu_0 = 1/\left(\chi_j^H\left(\coth\left(\chi_j^H H_1/h\right)+\coth\left(\chi_j^H H_2/h\right)\right)\right) \qquad (19)$$

which correspond to the Hankel transform of Green's function in spectral-domain analysis.

The normalized vector of current $\vec{I}$ is derived from the surface current density $\vec{k}(z)$ as follows:

$$\vec{I} = h[r_e]^{-1}[r]^{-1}\vec{k}(0). \qquad (20)$$

After transformation the reduced system of equations (18) takes the following form in the original domain:

$$\left(\vec{\vartheta}_s\right)_{\mathrm{red}} = \left([r]^{-1}[r_e][\Gamma_H][r_e][r]^{-1}\right)_{\mathrm{red}}\vec{i}_{\mathrm{red}} = [l_s]\vec{i}_{\mathrm{red}}. \qquad (21)$$

The elements dl_{ik}/ds of the real, symmetric matrix $[l_s]$ represent microinductances with respect to ds. In the same manner as the microcapacitances, these form a dense network, illustrated in Fig. 3(b) for the same structure as in Fig. 3(a).

Because of the perfect conductivity the normal component of induction vanishes on the strips at $z = 0$. As a consequence the vector potential must satisfy a homogeneous differential equation there, with the general solution $\varphi^H(0) = (\bar{\rho}/\rho)\hat{\varphi}$, where $\hat{\varphi}$ denotes the amplitude. For the discretized functions one obtains from (17) the relation $(\vec{\vartheta}_s)_{\mathrm{red}} = \hat{\vec{\varphi}}$. The magnetic flux with respect to ds on the strips can be arbitrary and is chosen to be unity, i.e., $\hat{\vec{\varphi}} = \vec{1}$.

After inversion of (21), summation of the inverse microinductances, and inversion of the resultant matrix, the following final equation for the macro- or stripline inductances is obtained:

$$\vec{\vartheta}' = [L_s]\vec{i} \qquad (22)$$

with the flux per unit length $\vec{\vartheta}' = (\vartheta_s^{①}, \cdots, \vartheta_s^{Ⓝ})^t$ and the corresponding currents $\vec{i} = (i^{①}, \cdots, i^{Ⓝ})^t$ on the N circular conductors.

In some methods the outer inductances are calculated using the inductance integral [8]. The self-inductances then represent improper integrals, which, for striplines with zero thickness, cause numerical problems. This difficulty does not exist if the inductances are calculated, as the capacitances are, from a partial differential equation.

In the present method a uniform solution of the static field problems is possible by means of two simple intermediate transformations, called normalization. The vectors of the original domain, e.g. $\vec{\varphi}^E, \vec{\varphi}^H, \vec{\vartheta}, \vec{q}$, are then transformed into the vectors of the "normalized" domain, characterized by capital letters, i.e., $\vec{\Phi}^E, \vec{\Phi}^H, \vec{\theta}, \vec{Q}$.

In the limit $\bar{\rho} \to \infty$ the curved transmission lines converge to the straight conductor system and if the magn. (el.) cylinder (Fig. 2) is replaced by an electric one with sufficiently large radius ρ_0 we have the relation

$$\lim_{\bar{\rho}\to\infty} l_j/\mu_0 = \left(c_j^0/\epsilon_0\right)^{-1} \qquad (23)$$

with the 0 denoting $\epsilon_{r1} = \epsilon_{r2} = 1$.

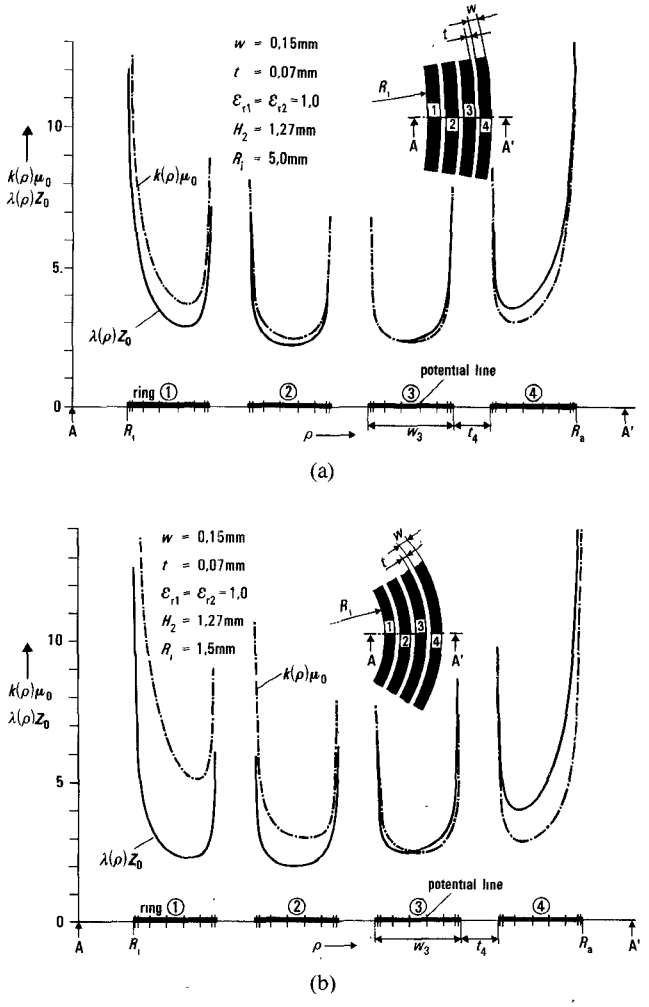

Fig. 4. The surface current density $k(\rho)$ and the charge density $\lambda(\rho)$ of a system of $N = 4$ circular microstrip rings ($\vec{u}/v_0 = \vec{\vartheta}' = \vec{1}$), where $w_n = w$ $(n = 1, \cdots, N)$ and $t_n = t$ $(n = 2,3,4)$; $\epsilon_{r2} = \epsilon_{r1} = 1$; and $v_0 = 1/\sqrt{\mu_0\epsilon_0}$. The markings on the abscissa give the locations of the potential lines and the conducting rings ① to ④ are indicated by large line widths. The density distributions are given for (a) $R_i = 5.0$ mm and (b) $R_i = 1.5$ mm.

In the original domain the following relation holds:

$$\lim_{\bar{\rho}\to\infty} [L_s]/\mu_0 = [L']/\mu_0 = \left([C_0']/\epsilon_0\right)^{-1} \qquad (24)$$

where $[C_0']$ gives the capacitance matrix in vacuum and $[L']$ the inductance matrix of the straight planar multiconductor system, treated in [12], [14].

As mentioned in the preceding section, the transmission properties of the curved multiconductor system are described by currents and voltages.

The two basic equations for the quasi-TEM analysis are derived from (16) and (22):

$$\frac{d}{ds}\vec{i} = -j\omega[C_s]\vec{u} \qquad \frac{d}{ds}\vec{u} = -j\omega[L_s]\vec{i} \qquad (25)$$

where $\vec{i}$ and $\vec{u}$ give the vectors of transmission line currents and voltages, respectively.

After differentiation with respect to s and substitution one obtains second-order differential equations for $\vec{i}$ and $\vec{u}$. The elements of $\vec{u}$ are coupled by the real but not symmetric matrix $[L_s][C_s]$.

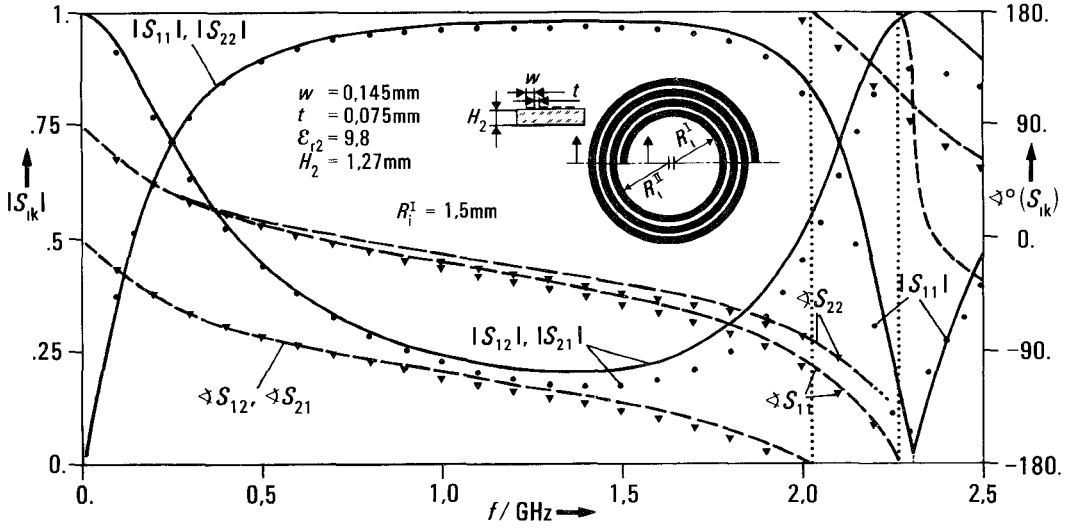

Fig. 5. Calculated (measured) S parameters of the two-port sketched in the figure: ---- (▼) for the phase and ——— (●) for the magnitude. Port 2 refers to the inner end of the spiral structure

Decoupling is achieved by a real transformation [15], which results in the following matrix equation:

$$\frac{d^2}{ds^2}\vec{V}+[\chi]^2\vec{V}=\vec{0} \tag{26}$$

with the vector of transformed voltages $\vec{V}(s)=[T_u]^{-1}\vec{u}(s)$ and the real eigenvalues $[\chi]=\mathrm{diag}(\chi_j)$.

A comparison of (11) with (26) reveals the relationship between the method of lines for determining the transverse fields and the conventional technique for calculating the wave propagation.

With [15] one obtains the matrix equation for the currents and voltages at the beginning and at the end of a circularly curved multiconductor system:

$$\begin{bmatrix}\vec{i}(s_a)\\ \vec{i}(s_b)\end{bmatrix} = Y_0([C_s]/\epsilon_0)[T_u]\left[\begin{array}{c|c}[y_{11}] & [y_{12}]\\ \hline [y_{21}] & [y_{22}]\end{array}\right][T_u]^{-1}\begin{bmatrix}\vec{u}(s_a)\\ \vec{u}(s_b)\end{bmatrix} \tag{27}$$

where $s_{a(b)}$ denote the two planes of the $2N$-port network, $Y_0=1/Z_0=\sqrt{\epsilon_0/\mu_0}$, and $[y_{11}]=[y_{22}]$, $[y_{12}]=[y_{21}]$ are diagonal matrices.

III. Results

The multiconductor system of Fig. 1 is composed of straight and circularly curved transmission lines. For large radii R_i and at low frequencies we have only a small distortion of the electromagnetic field due to curvature; i.e., the field is approximately TEM. The static distributions of the charge and the current density for $\vec{u}\sim\vec{\vartheta}'$ are then approximately proportional.

The charge density $\lambda(\rho)$, which is derived from $\vec{\lambda}=[r]^{-2}\vec{\sigma}$, and the surface current density $k(\rho)$ of a system of four circular striplines in a homogeneous dielectric ($\epsilon_{r1}=\epsilon_{r2}=1$) are depicted in Fig. 4(a). The inner radius of curvature is given by $R_i=5.0$ mm.

In the limiting case of straight lines, i.e., for $R_i=\infty$, the two sets of curves coincide and the fields are pure TEM at all frequencies. In that case we have exactly $d/ds\,u^{(n)}=-j\omega\vartheta_s^{(n)}$ and $d/ds\,i^{(n)}=-j\omega q_s^{(n)}$, where $u^{(n)}$ and $i^{(n)}$ denote unique line integrals for the nth stripline.

If the dielectric is layered, this uniqueness is lost and the quantity "current" or "voltage" has to be defined differently [15]. A graphical representation corresponding to Fig. 4 of the surface current density and the charge density for $R_i=\infty$ and $\epsilon_{r2}>1$ would show two different sets of curves, which are not simply proportional.

Hence from the static distributions we can deduce that an inhomogeneous dielectric and curvature both lead away from TEM.

For the same system of conductors as in Fig. 4(a) but with a smaller inner radius of curvature $R_i=1.5$ mm, the charge density and the surface current density are depicted in Fig. 4(b). With an increase of curvature the two distributions $\lambda(\rho)Z_0$ and $k(\rho)\mu_0$ become increasingly different, so that the largest difference is given for strip ①, as can also be deduced from (8).

The capacitance and the inductance matrices of the aforementioned four-conductor system with the geometrical parameters $w=0.15$ mm, $t=0.07$ mm, $H_2=1.27$ mm, $R_i=1.5$ mm, and $\epsilon_{r2}=9.8$ are given in the Appendix. As can be seen the outer diagonal elements of the real and symmetric matrices are different. In the limiting case of straight conductors they are equal.

The number of lines for the spacings t has been taken to be $M_{\min}=5$, so that after considering the edge condition [12], [13], four lines describe the static fields of the spacings. The matrices $[C_s]$ and $[L_s]$ have been calculated using $M=93$ lines.

For the shielding electrical walls the distances $H_1=10\cdot H_2$ and $\rho=R_a+5(R_a-R_i)$ have proved to be sufficiently large. Doubling these distances changes the ele-

ments of the matrices (A1) and (A2) (see the Appendix) by less than 0.5 percent.

If the number of lines $M_{\min}$ for the smallest distance, i.e., for t, is increased from $M_{\min}=3$ to $M_{\min}=7$ the capacitances and inductances change by less than 0.5 percent.

To show the effect of curvature in a quasi-TEM analysis, two curved multiconductor systems with four and three striplines are joined together. They form a two-port network similar to a circular spiral inductor. The structural data of the four-conductor system are $w=0.145$ mm, $t=0.075$ mm, $H_2=1.27$ mm, $\epsilon_{r2}=9.8$, $R_i^I=1.5$ mm, and $\alpha_0=\pi$. The same angle is given for the adjacent three-conductor system with the larger inner radius $R_i^{II}=(2R_i^I+w+t)/2$.

The S parameters of this structure, which is assumed lossless, are plotted versus frequency in Fig. 5. With increasing frequency the neglect of the radial component of the surface current and the diverse losses lead to an increasing discrepancy between the calculated and the measured results, especially for the magnitudes.

Since the measured values of $|S_{22}|$ differ only slightly from the measured $|S_{11}|$, they are not shown in the figure. The difference in the phase angles $\arc(S_{11})$ and $\arc(S_{22})$ corresponds to the difference of the outer capacitances in an equivalent circuit with discrete elements.

In the measurement setup the DUT, sketched in Fig. 5, is connected to intervening transmission lines by bond wires. These bond wires were examined individually and taken into account using a correction program.

IV. Conclusions

A quasi-TEM analysis for straight and weakly curved planar multiconductor transmission lines is presented. To show the accuracy of the approach, a two-port network similar to a spiral inductor has been calculated and measured.

The method of approximation is suited for analysis of microwave components as well as high-speed digital circuits with interconnections consisting of curved striplines instead of straight lines with discontinuities.

Appendix

Capacitance Matrix:

$$\begin{bmatrix} 11.189 & -6.028 & -1.117 & -0.647 \\ -6.028 & 16.106 & -6.278 & -1.254 \\ -1.117 & -6.278 & 18.085 & -7.599 \\ -0.647 & -1.254 & -7.599 & 15.800 \end{bmatrix} = [C_s]/\epsilon_0. \quad \text{(A1)}$$

Inductance Matrix:

$$\begin{bmatrix} 0.470 & 0.275 & 0.203 & 0.161 \\ 0.275 & 0.534 & 0.316 & 0.235 \\ 0.203 & 0.316 & 0.607 & 0.363 \\ 0.161 & 0.235 & 0.363 & 0.691 \end{bmatrix} = [L_s]/\mu_0. \quad \text{(A2)}$$

Acknowledgment

The author would like to thank F. Koppehele for his liberal encouragement. He is also grateful to Dipl.-Ing. L. Slawitschka for his valuable assistance in performing the measurements.

References

[1] L. Lewin, D. C. Chang, and E. F. Kuester, *Electromagnetic Waves and Curved Structures*. London: Peter Peregrinus, 1977.
[2] V. K. Tripathi and I. Wolff, "Perturbation analysis and design equations for open- and closed-ring microstrip resonators," *IEEE Trans. Microwave Theory Tech.*, vol. MTT-32, pp. 405–410, 1984.
[3] H. Buchholz, "Der Einfluss der Kruemmung von rechteckigen Hohlleitern auf das Phasenmass ultrakurzer Wellen," *E.N.T.*, Band 16, pp. 73–85, 1939.
[4] J. Meissner, "Radiation losses of *E*-plane groove-guide bends," *Electron. Lett.*, vol. 19, no. 14, pp. 527–528, 1983.
[5] E. A. J. Marcatili, "Bends in optical dielectric guides," *Bell Syst. Tech. J.*, pp. 2103–2132, 1969.
[6] I. Wolff and W. Menzel, "The microstrip double-ring resonator," *IEEE Trans. Microwave Theory Tech.*, vol. MTT-23, pp. 441–444, 1975.
[7] I. V. Lindell and G. Qizheng, "Theory of time-domain quasi-TEM modes in inhomogeneous multiconductor lines," *IEEE Trans. Microwave Theory Tech.*, vol. MTT-35, pp. 893–897, 1987.
[8] F. Ollendorff, *Calculation of Magnetic Fields*. (in German). Wien: Springer Verlag, 1952.
[9] O. A. Liskovets, "The method of lines (Review)," *Differentsial'nye Uravneniya*, vol. 1, no. 12, pp. 1662–1678, 1965.
[10] S. B. Worm and R. Pregla, "Hybrid-mode analysis of arbitrarily shaped planar microwave structures by the method of lines," *IEEE Trans. Microwave Theory Tech.*, vol. MTT-32, pp. 191–196, 1984.
[11] H. Diestel and S. B. Worm, "Analysis of hybrid field problems by the method of lines with nonequidistant discretization," *IEEE Trans. Microwave Theory Tech.*, vol. MTT-32, pp. 633–638, 1984.
[12] H. Diestel, "Analysis of planar multiconductor transmission-line systems with the method of lines," *Arch. Elek. Übertragung.*, vol. 41, no. 3, pp. 169–175, 1987.
[13] H. Diestel, "A uniform analysis of straight and circular planar multiconductor systems," *Arch. Elek. Uebertragung.*, vol. 42, no. 1, pp. 54–58, 1988.
[14] C. Wei, R. F. Harrington, J. R. Mautz and T. K. Sarkar, "Multiconductor transmission lines in multilayered dielectric media," *IEEE Trans. Microwave Theory Tech.*, vol. MTT-32, pp. 439–449, 1984.
[15] R. Briechle, "Uebertragungseigenschaften gekoppelter, verlustbehafteter Mehrleitersysteme mit geschichtetem Dielektrikum," *Frequenz*, vol. 29, Heft 3, pp. 69–79, 1975.

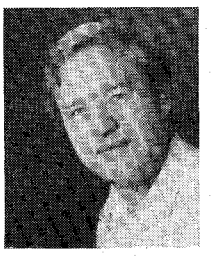

Heinrich Diestel was born in Haseluenne, Germany, on April 16, 1952. He received the Dipl.-Ing. degree from the Technical University Hannover, Germany, in 1978 and the Dr.-Ing. degree from the Fernuniversitaet in Hagen, Germany, in 1984.

Since 1984 he has been with SIEMENS AG, Munich, where he is engaged in the Computer-aided design of microwave and millimeter-wave integrated circuits. His interests include the application of various numerical methods.